Computer Life (CPL) ISSN: 1819-4818
DELIVERING QUALITY SCIENCE TO THE WORLD

Experimental investigation of laminates with different SMAs positions with Low-velocity impact

Xuana Gu, Zheng He[a, *], Xiaoyua Sun, Ju Liu, Binsheng Wang, Jianxin Teng

College of Aerospace and Civil Engineering, Harbin Engineering University, Harbin 150001

China

[a]hezheng@hrbeu.edu.cn

Abstract—The dynamic behavior of composite laminates is very complex because there are many concurrent phenomena during composite laminate failure under impact load. Fiber breakage, delaminations, matrix cracking, plastic deformations due to contact and large displacements are some effects which should be considered when a structure made from composite material is impacted by a foreign object. Thus, an investigation of the low velocity impact on laminated composite thin disks of epoxy resin reinforced by carbon fiber is presented. The influence of stacking sequence and energy impact was investigated using load–time histories, displacement–time histories and energy–time histories as well as images from NDE. Indentation tests results were compared to dynamic results, verifying the inertia effects when thin composite laminate was impacted by foreign object with low velocity. Finite element analysis (FEA) was developed, using Hill's model and material models implemented by UMAT (User Material Subroutine) into software ABAQUS™, in order to simulate the failure mechanisms under indentation tests.

Key words: Composite laminates, Low velocity impact, NDE; Indentation tests, Finite element analysis

---

1. INTRODUCTION

During the last years, criteria of automobile and aircraft projects have been more and more rigorous for component developed in order to absorb impact energy. Research on the development of structural components with high crashworthiness has been carried out not only by the automobile and aeronautics industries, but also by naval, trains and elevators industries. The project concept for structural components with high crashworthiness depends on the crash resistance concept described by Kindervater and Georgi [1]. The crash resistance concept is based on the energy absorption capacity and structural integrity. For developing a project that reaches these requirements, it should change the material and/or architecture of the component. However, changes in the architecture can cause increase of costs and/or of weights, reducing

the performance of the structure. The weight increase is not attractive for the aircraft development, because it reduces the aircraft performance. Nowadays, many kinds of components have been made using composite materials, because these materials can absorb a high amount of impact energy and can guarantee the survival of the passengers.

This work shows an experimental investigation and numerical results of the low velocity impact on thin composite laminates plates of epoxy resin reinforced (matrix) by carbon fiber (reinforcement). This study describes the technology to manufacture the specimens and the set-ups of equipment's to make dynamic experimental tests (using a drop-tower instrumented) and to realize non-destructive evaluation (NDE) (using ultrasonic C-scan), as well as the finite element model and UMAT subroutine implemented into software ABAQUS™ to simulate the failure mechanisms of the composite laminate. Afterwards, several issues are discussed:

Experimental results as load–time, displacement–time and energy–time histories of the laminate plate impacted under low velocity, considering different stacking sequence and different impact energies;

Experimental results as images from non-destructive evaluation (NDE) of laminate damaged after impact test, using NDE by ultrasonic C-scan technique;

Experimental results as load–displacement of the laminate under indentation test (quasi-static loading), considering the same stacking sequence used during impact test and the same maximum force level reached at impact tests;

Comparison between experimental results from impact and indentation tests;

Comparison between indentation tests results and finite element model results, using Hill's model and two material models implemented by UMAT.

2. EXPERIMENTAL

The intra-ply damage at fibers is shown by mechanism 4 (Fig. 1) that is the fiber rupture. However, the fiber failure mode depends on the type of loading, because compression loads can induce micro-buckling, but tensile loads can induce rupture of fibers. The intra-ply damage at the matrix depends on the ductility of the polymer, as well as on the in-service temperature. Thus, the polymeric matrix can present a fragile or a plastic behavior (mechanism 5).

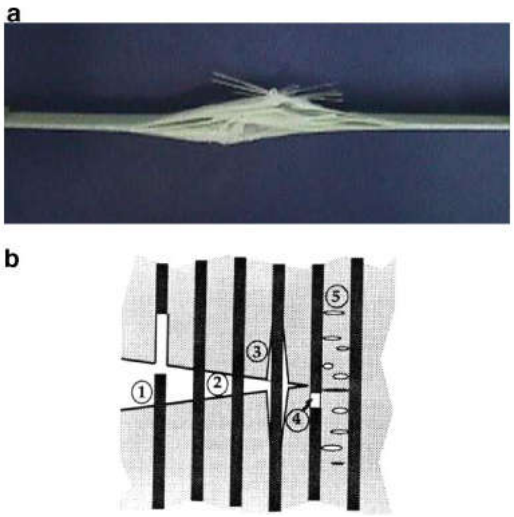

Fig. 1 (a) Composite failure mechanisms: intra-ply and inter-ply failures and (b) Intra-ply damages (by Anderson[2]).

After the hand-lay-up process used to stack the plies, the composite plate was put in the auto-clave with vacuum system set to −0.8 Bar (−0.08 MPa). According to Hexcel®, the complete cure cycle for M10 occurs when this material is processed at 120 °C, under a pressure with range from 0.3 to 5.0 Bar for 60 min (Fig. 2). After the curing process, the composite plates were cut on square shapes (length and width of 120 mm and thickness of 1.8 mm), using diamond saw in order to guarantee the tolerances specified by standards.

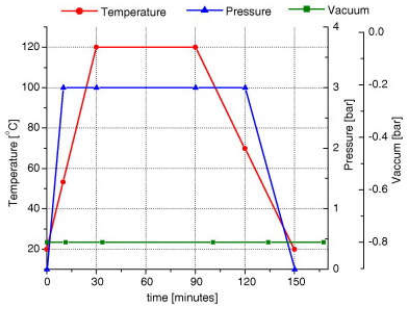

Fig. 2 Cure cycle.

The instrumented drop-tower has an optic sensor fixed at the base and a LED ("light emitting diode") attached to the support of the mass, which permits to measure the displacement of the impactor support in function of the time ($s_i(t)$) shown in Fig. 3. Thus, numerical methods to derive the displacement measured were applied in order to obtain the velocity ($v_i(t)$) and acceleration of the support during the impact event. On the other hand, the load cell measures the force during the impact event ($F_{exp}(t)$) shown in Fig. 3. The load cell was plugged on a Kistler™ amplifier (model 5007) that sends signal to the computer. In the computer, there is a system for data acquisition with 11 bits, three channels for input data and

sampling frequency set to 19 kHz. Thus, the acceleration of the load cell was obtained dividing the force measured by the impact mass.

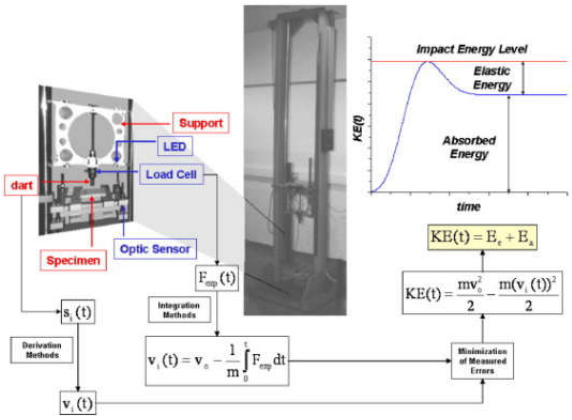

Fig. 3 Drop-tower at LCPC of Katholieke Universiteit Leuven: kinematic energy (impact energy level), absorbed energy and elastic energy.

Fig. 4 shows the E_{11} degradation law for Chang and Chang[3-4] and for the present work, where β is the Weibull distribution parameter. The parameter H is similar to parameterβ. Thus, it is not verified that the Young modulus reduces suddenly, which is very reasonable for indentation tests.

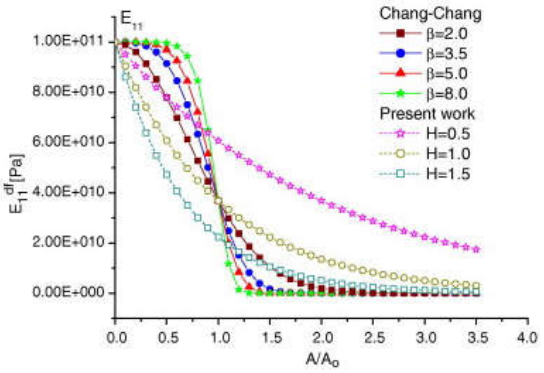

Fig. 4 $E11$ degradation laws.

For the finite element analysis, two types of finite element models were developed. The first model was created using shell elements (S4) with four nodes and four integration points [5]in order to simulate the plane stress at the laminate. The nodes at the edge of the model were fixed in order to simulate the circular disk clamped (Fig. 5a). The second model was created, using solid elements (C3D8) with eight nodes and four integration points in order to simulate the 3D state of stress at laminate. The solid had three elements per thickness and the nodes at the edge of the model were fixed (Fig. 5b). It is important to note that for the shell model, as well as for

the solid model, the external surface of the indention hemisphere was simulated as a rigid surface, which contacted the central region of the disk.

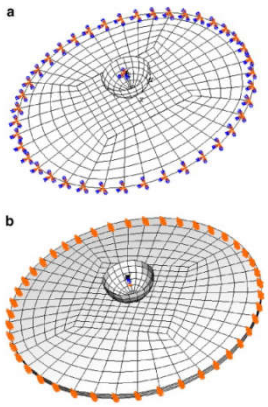

Fig. 5 Finite element models: (a) Shell element S4 and (b) Solid element C3D8.

Fig. 6 shows that the software ABAQUS™ manages all calculation procedures, and the user can recover components of the stress tensor for each iteration *i*. After that, the stress tensor for each integration point is read by the UMAT subroutine in order to be used in a failure criterion. If failure does not occur, then the updated stress tensor is equal to the original stress tensor. Thus, this tensor comes back to the principal calculus procedure in order to form the internal forces vector, which will be compared to the external forces vector. The result of this comparison will produce residues (*R*) that will be compared to a specified tolerance. If *R* is higher than the tolerance, a new iteration will be necessary.

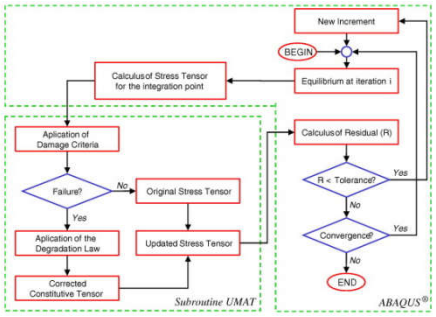

Fig. 6 UMAT subroutine and software ABAQUS™.

3. RESULTS AND DISCUSSION

Fig. 7 a shows force–time graphics for composite plates with stacking sequence $[0]_{10}$, considering two impact energy levels (5.91 J and 2.36 J). There is a region with oscillations of high frequency (in the initial phase of contact from 0 to 1 ms) due to initial contact between specimen and dart at force–time graph (Fig. 7a).Fig. 7b shows the energy–time graph for

composite plates with stacking sequence $[0]_{10}$, considering the impact energy of 5.91 J. Based on Fig. 3 , it is verified that specimens have absorbed energy equal to 4.42 J, so only 25% of the impact energy is converted to elastic vibrations.

Fig. 8 shows the ultrasonic C-scan images for composite plates with stacking sequence $[0]_{10}$, considering the impact energies of 5.91 J and 2.36 J. Specimens impacted by 5.91 J show damage more concentrated close to the impact region (Fig. 8a). However, specimens impacted by 2.36 J show damage more distributed at the matrix represented by cracks oriented to the fibers (Fig. 8b). Besides, it was observed that some fibers fail at the opposite side of the impact for the specimens impacted at 5.91 J. This observation can explain why these specimens absorbed 75% of the impact energy, where the failure mechanisms of fibers release more energy than failure mechanisms of the matrix. Because the energy to rupture the fibers is higher than the energy to crack the polymer matrix.

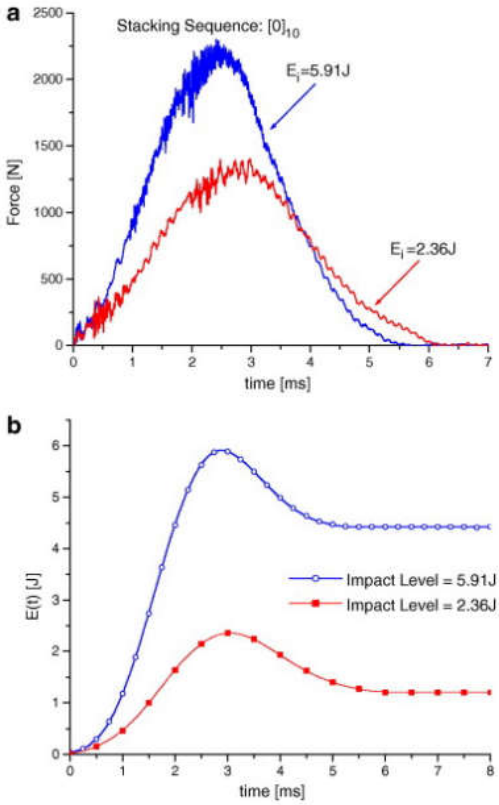

Fig. 7 Experimental impact results for laminate [0]10.

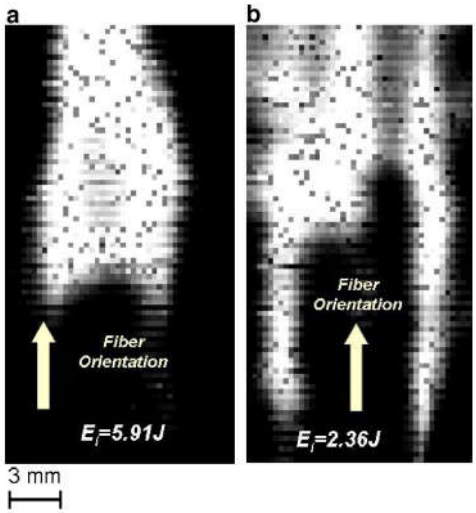

Fig. 8 Experimental impact results for laminate [0]10: (a) energy–time for 5.91 J and 2.36 J and (b) C-scan images.

Fig. 9 a shows force–time graphics for composite plates with stacking sequence $[0/90/0/90/0]_s$, considering two impact energy levels (5.91 J and 2.36 J).There is a region with oscillations of high frequency (from 0 to 1.2 ms) due to initial contact between specimen and dart in the force–time graph (Fig. 9a). Fig. 9b shows the energy–time graph for composite plates with stacking sequence $[0/90/0/90/0]_s$, considering the impact energy of 5.91 J. It is verified that specimens have absorbed energy of 3.96 J, so only 33% of the impact energy is converted to elastic vibrations. However, the specimens impacted by 2.36 J have just 0.58 J for absorbed energy (Fig. 9b), converting 75% of the impact energy to elastic vibrations.

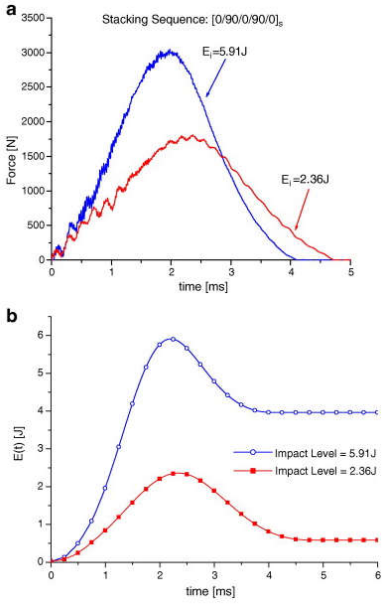

Fig. 9 Experimental impact results for laminate [0/90/0/90/0]s.

Fig. 10 shows the ultrasonic C-scan images for composite plates with stacking sequence $[0/90/0/90/0]_s$, considering the impact energy of 5.91 J (Fig. 10a) and 2.36 J (Fig. 10b). Due to the stacking sequence $[0/90/0/90/0]_s$, there are more layers oriented at 0° than at 90°, so, there are more cracks aligned to 0°. Besides, there are "peanut shapes", which represent delaminations, at both directions (0° and 90°). The area damaged for the specimens impacted by 5.91 J (340 mm^2) is larger than the specimens impacted by 2.36 J (150 mm^2). This calculus can explain why the specimens impacted by 2.36 J absorbed just 25% of the impact energy. Many failure mechanisms cannot be activated for the stacking sequence equal [0/90/0/90/0] by this impact energy level, and the mechanical behavior of the specimen tends to elastic response.

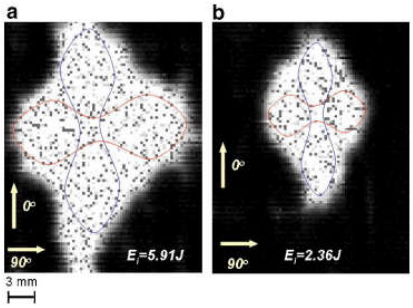

Fig. 10 Experimental impact results for laminate [0/90/0/90/0] s: (a) energy–time for 5.91 J and 2.36 J and (b) C-scan images.

Fig. 11 shows force–time graphs for composite plates with stacking sequence [+45/−45/+45/0/90] , considering four impact energy levels (2.36 J, 4.33 J, 5.91 J and 10.82 J).

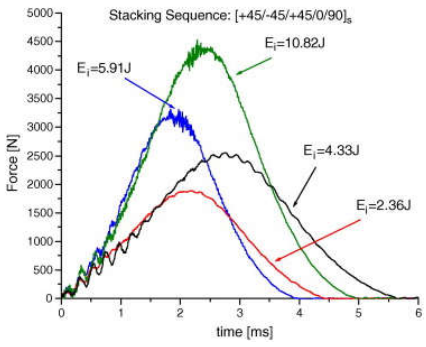

Fig. 11 Experimental impact results for laminate [+45/−45/+45/0/90] s.

Fig. 12 shows the energy–time graph for composite plates with stacking sequence $[+45/-45/+45/0/90]_s$, considering the impact energy equal to 5.91 J. Specimens have absorbed 4.0 J of energy, so only 32% of the impact energy is converted to elastic vibrations.

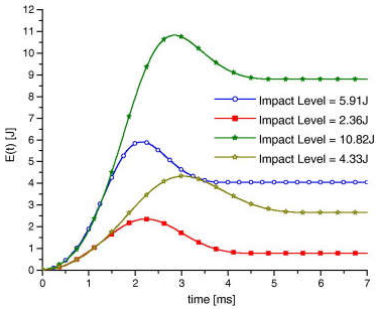

Fig. 12 Experimental impact results for laminate [+45/−45/+45/0/90] s Energy–time for 5.91 J; 2.36 J; 10.82 J; 4.33 J.

Fig. 13 shows the ultrasonic C-scan images for composite plates with stacking sequence $[+45/-45/+45/0/90]_s$, considering the impact energy levels of 5.91 J (Fig. 13a), 2.36 J (Fig. 13b), 10.82 J (Fig. 13c) and 4.33 J (Fig. 13d).

Fig. 14 shows the force–displacement graphs for composite plates with stacking sequence $[0]_{10}$. In general, in the initial phases of loading, the indentation and the impact curves have about the same slope that represents non-linear behavior due to the contact phenomenon.

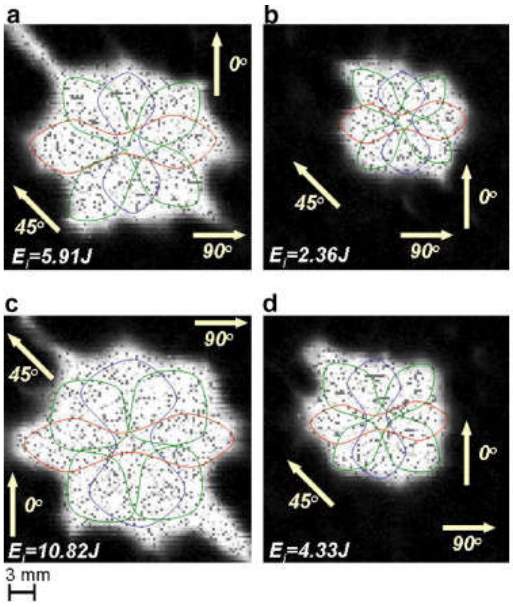

Fig. 13 Experimental impact results for laminate [+45/−45/+45/0/90] s: C-scan images.

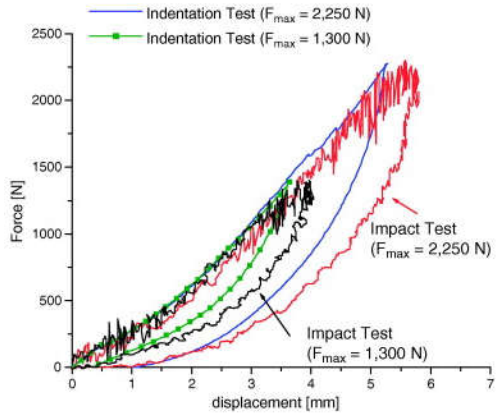

Fig. 14 Experimental indentation results for laminate [0]10 maximum force at: 2250 N and 1300 N.

Fig. 15 shows the force–displacement graphics for composite plates with stacking sequence $[0/90/0/90/0]_s$. In general, in the initial phases of the loading step, the indentation and the impact curves have about the same slope that represents non-linear behavior due to the contact interaction between the disks and the aluminium dart (hemisphere).

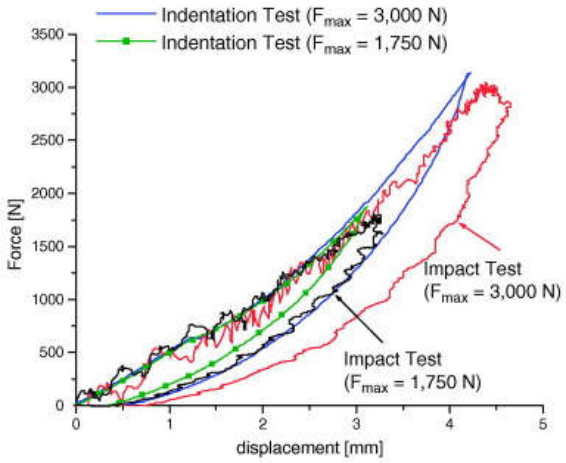

Fig. 15 Experimental indentation results for laminate [0/90/0/90/0] s maximum force at: 3000 N and 1750 N.

Fig. 16 shows the force–displacement graphs for composite plates with stacking sequence $[+45/-45/+45/0/90]_s$. Fig. 16 shows that the indentation and the impact curves have different slopes. The specimens with stacking sequence $[+45/-45/+45/0/90]_s$ impacted show many types of failure mechanisms that are distributed at composite plate.

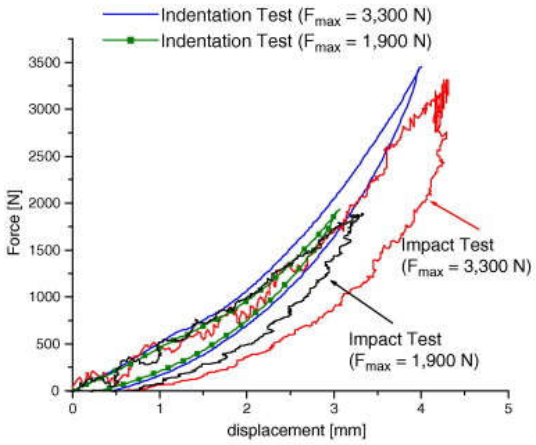

Fig. 16 Experimental indentation results for laminate [+45/−45/+45/0/90] s maximum force at: 3300 N and 1900 N.

Fig. 17 a show that the Material Model I can simulate the indentation test, during the loading phase when parameter *H* is 1.2. However, the maximum load simulated is higher than the experimental maximum load, and, the initial phase of unloading is not simulated very well. Material Model I can simulate the final of phase unloading, but the permanent strain is not represented when the polymer matrix exhibits plastic deformation under the rigid hemisphere. This phenomenon can be verified inFig. 17b, that shows a stress concentration at the centre of the disk, because the contact interaction between the disk and the rigid hemisphere causes contact press and contact stress.

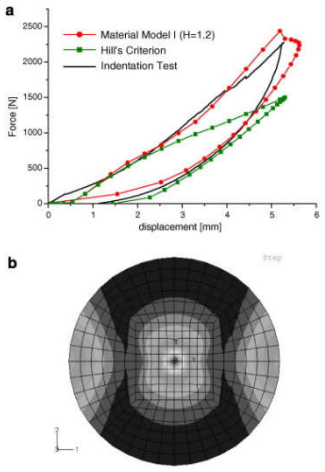

Fig. 17 Numerical indentation results for laminate [0]10: (a) force–displacement and (b) stress distribution.

Fig. 18 shows that the Material Model I can simulate the indentation test, during the loading and unloading phases when parameter *H* is equal to 1.6. Besides, the maximum load simulated is quite similar to the experimental maximum load. Fig. 18 shows that Material Model II can

simulate the indentation test during the loading and unloading phases, when parameter H is set to 0.4. Correlation with experimental results is better than with Material Model I.

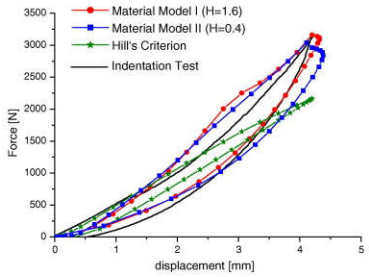

Fig. 18 Numerical indentation results for laminate [0/90/0/90/0] s.

Fig. 19 shows that Material Model I cannot simulate the indentation test very well, during the loading and unloading phases when parameter *H* is 1.2. Fig. 19 shows that Material Model II cannot simulate very well the indentation test during the loading and unloading phases, when parameter *H* is equal to 0.3, because the non-linear behavior caused by the shear stresses is not simulated with accuracy.

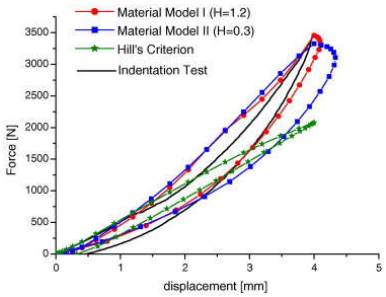

Fig. 19 Numerical indentation results for laminate [+45/−45/+45/0/90] s.

4. CONCLUTION

For the experimental approach, it is verified that stacking sequence and impact energy level can influence on the dynamic response of composite plates. The graphs of force–time and energy–time, as well as the images from ultrasonic C-scan technique are used in order to compare the mechanical behavior of the specimens, which is represented by graph of the absorbed energy versus impact energy level. Fig. 20 can be divided into three regions:

Region 1: the specimens have a quasi-elastic behavior, because the fraction of absorbed energy is very low (under 35%) as failure mechanisms are not activated;

Region 2: the specimens show some failure mechanisms, which are matrix crack and delaminations; so, the fraction of absorbed energy is intermediate between 35% and 75%;

Region 3: the specimens show many types of failure mechanisms, for example: fiber rupture, matrix crack and delaminations; so, the fraction of absorbed energy is very high (over 75%).

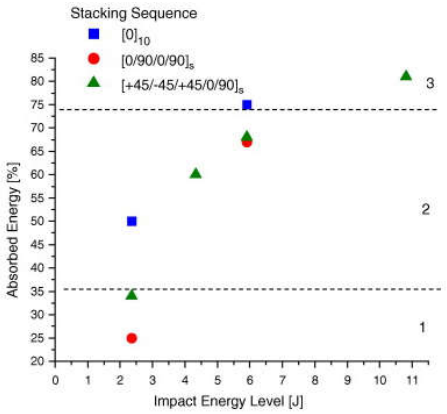

Fig. 20 Absorbed energy × impact energy.

ACKNOWLEDGEMENTS

This work is supported by the National Natural Science Foundation of China（No. 11602066）and the National Science Foundation of Heilongjiang Province of China (QC2015058 and 42400621-1-15047), the Fundamental Research Funds for the Central Universities.

REFERENCES

[1] C.M. Kindervater, H. Georgi Composite strength and energy absorption as an aspect of structural crash resistance J. Norman, W. Tomaz (Eds.), Structural crashworthiness and failure, Elsevier Science, London (1993), pp. 189–235.

[2] T.L. Anderson Fracture mechanics – fundamentals and applications CRC Press, New York (1995).

[3] F.K. Chang, K.Y. Chang Post-failure analysis of bolted composite joints in tension or shear-out mode failure J Compos Mater, 21 (9) (1987), pp. 809–833.

[4] F.K. Chang, K.Y. Chang A progressive damage model for laminated composites containing stress concentrations J Compos Mater, 21 (9) (1987), pp. 834–855.

[5] ABAQUS. Standard user's manual: theory. Pawtucket: Hibbitt, Karlsson & Sorensen, 2002.